

FLOW INVESTIGATION FOR SINGLE STAGE TURBINE CASCADE
USING FINITE DIFFERENCE NUMERICAL TECHNIQUE

Adnan ÖZTÜRK & Ali PINARBASI

Cumhuriyet University,
Eng.Fac. Mech. Eng. Dept.,
Sivas,TURKEY

ABSTRACT

In this study, the rotor and the stator for a axial turbine has been investigated using a computational technique. The method adopts a stream function vorticity approach and uses an Alternate Direction Implicit Technique to march vorticity, and a successive over-relaxation technique to obtain the stream function level. Flow assumed as steady, incompressible and viscid which adopted to 2-dimensional geometry. Initial calculations are presented the cascade blades for Reynolds numbers at 100, 1000 and 10000. Numerical results presented as stream function and 2-D velocities.

The results show that the flow through a diffusing, at single stage turbine cascade is strongly influenced by circumferential velocity. This effect is clearly discernable at the beginning of the time for the turbine cascade and decrease step by step. The passage wake and the blade trace effect have been observed within the turbine blades but it is increased the wake size. The secondary flow occurred at the leading edge of the rotor side. Presented data also explained that how strong generate the vortices within the turbine blades which estimated to be beneficial for CFD study when turbulence investigation needs to the turbine cascades.

INTRODUCTION

In rotating machinery of the radial turbine flow type, a variety of complex flow phenomena can be present. The structure of flow depends on the geometrical configurations of rotor and stator blades in addition to the usual flow parameters of Reynolds number, the gap of between the blades, flow structure etc.. In recent times, this complex turbine flows has received much attention especially use of computational technique. This is primarily due to the fact that there has been established which might offer an accurate and reliable method for investigation of flow behaviour at the turbine inlet.

Historically, many of fundamentals developments in such as complex flow at the turbine stage were published using a different techniques. Relaxation methods were developed when they were used in a cyclic formulation and adapted to fast digital computers. Chow (1970) studied 2-D

incompressible shear flow. The first major breakthrough was made by Yoshihara (1973), who demonstrated that solutions for two-dimensional, inviscid, transonic flow fields could be computed using finite difference algorithms programmed to run on digital computers. Effects of leaning and curving of its low aspect ratio and turning angle on the aerodynamic characteristics of turbine were shown experimentally by Wanjin et al.(1994). The centrifugal compressor, cascade aerodynamics were experimented by Pinarbasi and Johnson (1994, 1996) to investigate flow phenomena at diffuser resulted strongly that the blade trace was effected in the compressor. It was also made an experimental work by Yamamoto (1995) to investigate on interaction phenomena occurring between upstream and downstream cascade.

In the present study, loss generation occurring at the axial turbine stage were investigated numerically in a simple way to use the finite difference technique at various Reynolds numbers, based on the stream function-vorticity formulation of the steady incompressible Navier Stokes equations.

Numerical Method

The governing equations for the steady incompressible Navier Stokes equation are written which chosen by stream function/vorticity formulation. The first governing equation of fluid motion of mass is known as the continuity equation which is given by

$$\frac{\partial u}{\partial x} + \frac{\partial v}{\partial y} = 0 \quad (1)$$

where u and v are the x and y components of velocity, respectively. The stream function, ψ (x,y) is defined as,

$$u = \frac{\partial \psi}{\partial y}, \quad v = -\frac{\partial \psi}{\partial x} \quad (2)$$

$$u \frac{\partial u}{\partial x} + v \frac{\partial u}{\partial y} = \frac{1}{\rho} \frac{\partial p}{\partial x} \quad (3)$$

$$u \frac{\partial v}{\partial x} + v \frac{\partial u}{\partial y} = \frac{1}{\rho} \frac{\partial p}{\partial y} \quad (4)$$

$$\frac{\partial u}{\partial y} - \frac{\partial v}{\partial x} = 0 \quad (5)$$

The second governing equation of fluid motion, expressing the conservation of momentum, is the Euler equation which is written by following form for x and y components, and for a curl free two-dimensional velocity field expressed as, the velocity potential may be written as the gradient of a scalar potential $\phi(x,y)$

$$u = -\frac{\partial \phi}{\partial x}, \quad v = -\frac{\partial \phi}{\partial y} \quad (6)$$

substituting the definition of equation (6) into equation (1) gives,

$$\nabla^2 \phi = 0 \quad (7)$$

and substituting the definition of stream function in equation (2) into equation (5) gives,

$$\nabla^2 \psi = 0 \quad (8)$$

Stream function and vorticity method

The stream function/vorticity method has been used widely by many researchers, particularly for flow around circular cylinder (Lin et al (1976)). The momentum equation at x and y co-ordinate altered to allow for viscosity effect then equation become as equations (9) and (10),

$$\frac{\partial p}{\partial x} + \rho u \frac{\partial u}{\partial x} + \rho v \frac{\partial u}{\partial y} = \mu \left(\frac{\partial^2 u}{\partial x^2} + \frac{\partial^2 u}{\partial y^2} \right) \quad (9)$$

$$\frac{\partial p}{\partial y} + \rho u \frac{\partial v}{\partial x} + \rho v \frac{\partial v}{\partial y} = \mu \left(\frac{\partial^2 v}{\partial x^2} + \frac{\partial^2 v}{\partial y^2} \right) \quad (10)$$

introducing the vorticity term gives,

$$\frac{p_x}{\rho} - \psi_y \psi_{xy} + \psi_x \psi_{yy} = \nu \Omega_y \quad (11)$$

$$\frac{p_y}{\rho} - \psi_y \psi_{xx} + \psi_x \psi_{xy} = \nu \Omega_x \quad (12)$$

Eliminating the pressure term and writing the equation as differential form as below,

$$\psi_y \Omega_x - \psi_x \Omega_y = \nu \nabla^2 \Omega$$

$$\psi_x \Omega_y - \psi_y \Omega_x + \nu \nabla^2 \Omega = 0 \quad (13)$$

$$\psi_y (\nabla^2 \psi)_x - \psi_x (\nabla^2 \psi)_y = \nu \nabla^4 \psi \quad (14)$$

Above equations, we could write as a finite difference form of as below,

$$Re_{\Delta x} = \frac{\psi_N - \psi_S}{\Delta y} \frac{\Delta x}{\nu} = \frac{u \Delta x}{\nu} \quad (15)$$

$$Re_{\Delta y} = \frac{\psi_E - \psi_W}{\Delta x} \frac{\Delta y}{\nu} = \frac{u \Delta y}{\nu} \quad (16)$$

The vorticity Ω is defined by,

$$\Omega = \frac{\partial u}{\partial y} - \frac{\partial v}{\partial x} = \frac{\partial^2 \psi}{\partial x^2} + \frac{\partial^2 \psi}{\partial y^2} = \nabla^2 \psi \quad (17)$$

replacing u,v in the momentum equations by using equation (2) gives

$$\frac{p_x}{\rho} - \psi_y \psi_{yy} - \psi_x \psi_{yy} = \nu (\psi_{xxy} + \psi_{yyy}) \quad (18)$$

$$\frac{p_y}{\rho} - \psi_y \psi_{xx} + \psi_x \psi_{xy} = \nu (\psi_{xxx} + \psi_{xyy}) \quad (19)$$

and writing the stream function and vorticity as a differential form of numerical solution, where, Ω and ψ are the vorticity and stream function.

Equations (19) and (20) are solved by using a Gauss Seidal over relaxation method. For the boundary conditions are needed around the perimeter of the considered area. The stream

$$\Omega_c = \frac{\psi_W + \psi_E - 2\psi_C}{(\Delta x)^2} + \frac{\psi_N + \psi_S - 2\psi_C}{(\Delta y)^2} \quad (20)$$

$$\psi_C = \frac{\frac{\psi_W + \psi_E}{(\Delta x)^2} + \frac{\psi_N + \psi_S}{(\Delta y)^2} - \Omega_c}{\frac{2}{(\Delta x)^2} + \frac{2}{(\Delta y)^2}} \quad (21)$$

function (ψ) boundary condition can be obtained from a Taylor series expansion to give to second order,

$$\frac{\partial \psi}{\partial x} \left(x - \frac{\Delta x}{2}, 0 \right) = \frac{\psi(x,0) - \psi(x - \Delta x, 0)}{\Delta x} \quad (22)$$

This provides an expression for ψ on the boundary,

$$\psi(x,0) = \psi(x - \Delta x,0) - \Delta x \frac{\partial \psi}{\partial x} (x - \frac{\Delta x}{2}, 0) \quad (23)$$

To develop the vorticity (Ω) boundary condition, similar approach has been used as successfully applied by Bryan (1963) and Greenspan (1969).

$$\Omega(x,0) = \frac{2\psi(x,0) - \psi(x + \Delta x,0) - \psi(x - \Delta x,0)}{\Delta x^2} - \frac{2\psi(x,\Delta y) - \psi(x,0) - \psi(x,2\Delta y)}{\Delta y^2} \quad (24)$$

Grid generation

The density and distribution of grid points determines the accuracy of subsequent boundary calculations. A simple method is used to generate the calculating grid, which described by Amsden and Hirt (1973). For each iteration, the boundary points are moved a short distance along a straight line connecting the initial and final locations.

$$x_{i,j} = \frac{1}{8}(x_{i+1,j} + x_{i-1,j} + x_{i,j-1} + x_{i,j+1} + x_{i+1,j+1} + x_{i-1,j+1} + x_{i+1,j-1} + x_{i-1,j-1}) \quad (25)$$

This is the same as solving the following Laplace equations

$$\frac{\partial^2 y}{\partial S_1^2} + \frac{\partial^2 y}{\partial S_2^2} = 0 \quad (26)$$

$$\frac{\partial^2 y}{\partial S_1^2} + \frac{\partial^2 y}{\partial S_2^2} = 0 \quad (27)$$

In this study, grid generation were produced using 100x80 mesh points. Similarly, as explained above the mesh generated for the cascade blades which is shown in Figure 1.

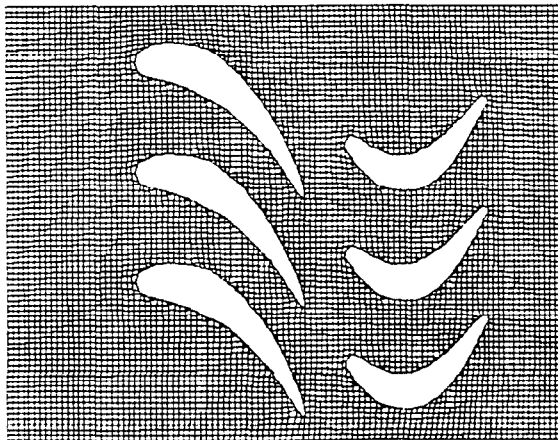


Figure 1 Grid Generation for Turbine Cascade

Numerical Results

To investigate rotor-stator interaction at a single stage turbine were computed using the finite difference technique. The computational results were presented as a stream function and 2-D velocities at various Reynolds number of 100, 1000 and 10000. Flow for viscid calculation were pictured by assuming steady flow during the path.

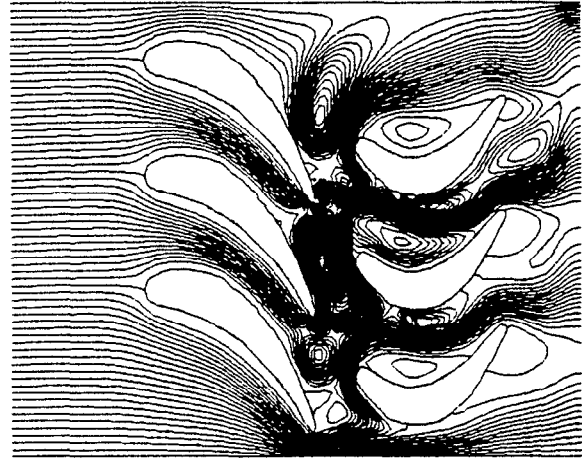


Figure 2a

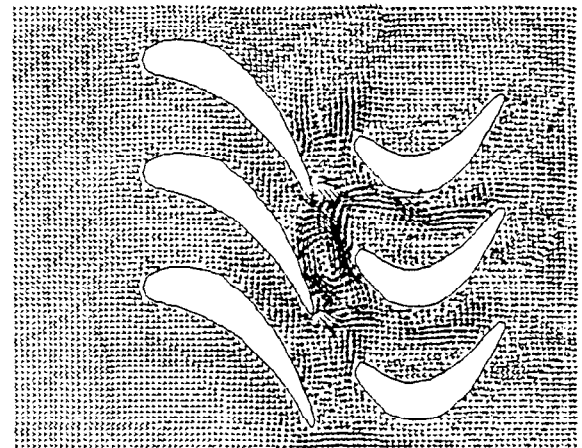


Figure 2b

Figure 2 Distribution of (a) the stream function and (b) 2-D velocity on the rotor-stator cascade at Reynolds number of 100

Figure 2 shows a typical results obtained at Reynolds number of 100 which consists steam function at Figure (2a) and 2-D velocities at Figure (2b). At both the cascade inlet and outlet, the passage vortices are seen to generate from the upstream and the downstream cascades. In the steady multiple-blade-row calculation, the stator and the rotor flow fields

are specified as a the inflow condition. This inflow condition shows that the main mixing flow are established at the trailing edge of the stator and the leading edge of the rotor. This effect of the blade interaction are seen clearly within the stator and the rotor. Figure (2a) shows that the passage vortices effect starts just only spanwise direction of the rotor by less influenced from the rotor interaction. This is due to less effect of Reynolds number and also fluid are expanding between the rotor blades.

The comparisons in Figures (2a) and (2b) indicate that there is much evidence about the passage vortices and the blade interaction effect on the turbine cascade which also traceable at 2-D velocity vectors. Main velocity at the leading edge of the stator were obtained rather higher than the rest of the passage and also its direction were seen parallel to the stator plane. This is expected result that may be due to the effect of the blade trace. A conclusion might be tell for this the stator and the rotor interaction part, the energy losses could be higher then which is shown at the passage vortex. This phenomena of the flow physics was also reported by Yamamoto et al. (1995) and is supported with it's measurements.

In order to simulate complex flow at the cascade, Reynolds number of 1000 were picture at Figure 3a and 3b, for stream function and 2-D velocities respectively. Comparing Figure 2 and Figure 3, it can be seen that the flow is expanding within the stator and the rotor blades. Both Figure 3a and 3b clearly explained that the wake development starts at the passage of the rotor. This is led to interaction between the vortex and the wake seems to decay the wake faster up to about midspan of the axial chord. After that the secondary flow starts to the leading edge of the rotor side. The passage wake has been spreading over the pressure side of the rotor and also the blade trace has lost effectiveness slowly where Reynolds number of 1000 by comparing Figure 2. This is indicate that when the Reynolds number higher, the higher loss prediction appeared especially within the stator and the rotor blades. This is also seen 2-D velocity pictures at Figure 3b. Vortex core accumulated at the trailing edge of the stator with high distributions. The region near the vortex is magnified for clarity at Figure 3b. Despite all, the suction side of the leading edge, vortex cannot be found in the turbine passage. The vortex may have merged quickly with the passage secondary flow or been dissipated by the viscous effect on the decay of the wake downstream of the turbine.

Figure 4 indicate that when Reynolds number of 10000 the passage wake still discernible with increasing of the core size. The location of the wake has covered at the same region of which is close to the pressure side of the rotor. The core size has increased intensively within this region. The

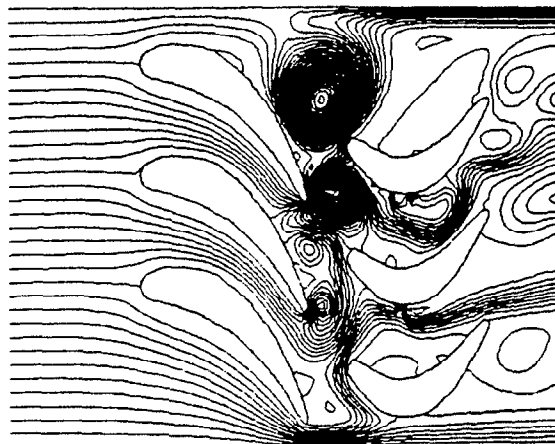


Figure 3a

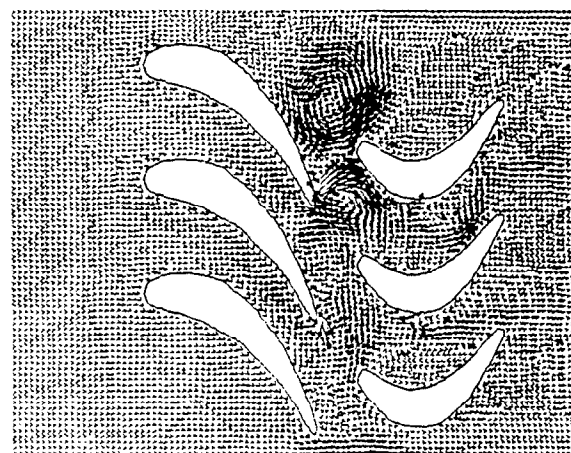


Figure 3b

Figure 3 Distribution of (a) the stream function and (b) 2-D velocity on the rotor-stator cascade at Reynolds number of 1000

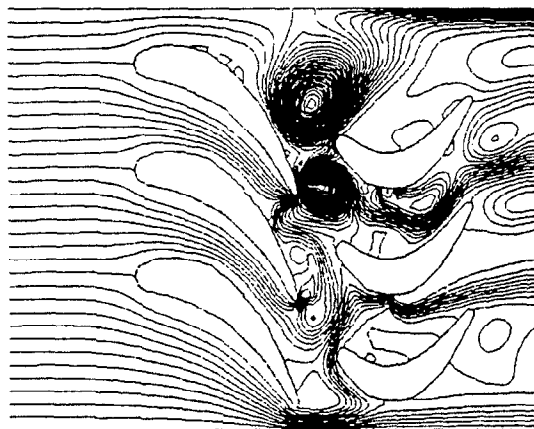


Figure 4a

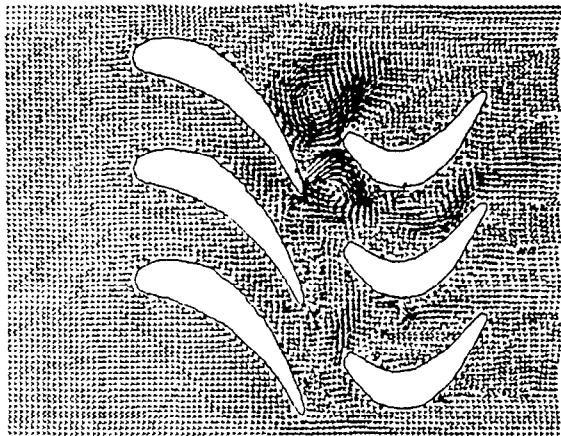


Figure 4b

Figure 4 Distribution of (a) the stream function and (b) 2-D velocity on the rotor-stator cascade at Reynolds number of 10000

to decay the wake faster compared to the wake decay at the lower Reynolds number. However, it merges with the wake as it travels downstream and becomes distinguishable from 2-D velocity vectors at Figure 4b.

Conclusions

It has been shown that the flow through a diffusing, at single stage turbine cascade is strongly influenced by circumferential velocity. The passage wake and the blade trace effect have been observed within the turbine blades but it is increased the wake size with higher Reynolds number, whereas the secondary flow occurred at the leading edge of the rotor side. Presented data explained that how strong generate the vortices within the turbine blades. This data can be used for CFD study when turbulence investigation needs to the turbine cascades.

REFERENCES

- Amsden, A.A., and Hirt, C.V., "A Simple Scheme for Generating General Curvilinear Grids", Journal Comp. Phys., Vol.11, p348, 1973
- Bryan, K., Journal Atoms Sciences, Vol.20, pp 594-606, 1963
- Chow, F., J. Aircraft, 7, pp 531-37, 1970
- Greenspan, D., "Numerical Study of Prototype Cavity Flow Problems", Comput. Journal, Vol.12, pp 89-96, 1969
- Lin C. L., Pepper D. W. and Lee S. C. "Numerical methods for separated flow solution around a circular cylinder" AIAA Journal, 14, 7, 900-907, 1976
- Pinarbasi A., Johnson MW., "Detailed Flow Measurements in a Centrifugal Compressor Vaneless Diffuser" ASME Turbo Expo Conference,

Pinarbasi A., Johnson MW., "3-D Flow Measurements in Conical and straight wall Centrifugal Compressor Vaneless Diffuser" Journal of Mechanical Engineering Science, Vol. 210, pp 51, 1996

Wanjin, H. et al., "Effects of leaning and curving of blades with high turning angles on the aerodynamic characteristics of turbine rectangular cascades" ASME Journal of Turbomachinery, Vol. 116, pp 417-424, 1994

Yamamoto, A., Murao, R., Suzuki, Y., Aoi, Y., "A Quasi-Unsteady Study on Wake Interaction of Turbine Stator and Rotor Cascades" ASME Journal of Turbomachinery, Vol. 117, pp 553-561, 1995

Yoshihara, H., AGARD-LS64, 1973